Therefore the sign conventions are opposite. In fluorine NMR the three-bond coupling constants for fluorines attached to olefins are consistently greater for the trans isomer than for cis isomer, and where sign information has been obtained, the sign of J for the trans isomer is negative but the sign of J for the cis isomer is positive.[26] Thus for fluorine coupling constants the signs of J for the cis and trans isomers are opposite and reversed from the signs of the EPR coupling constants reported here. For a variety of other nuclei it has also been observed that for 3- and 4-bond couplings across an olefinic linkage, the coupling constant is greater for the trans isomer than for the cis isomer.[27-30] Since the EPR couplings are through 10 bonds, there are undoubtedly many other factors that influence the magnitude of J than just the conformation of the olefin; however, it appears that the effect of the olefinic linkage on the magnitude of the EPR coupling constants parallels the effect of the same linkage on NMR couplings.

It has been stated that the value of J decreases exponentially with increasing values of r.[31,32] An exponential dependence of exchange on r is also assumed in fluorescence energy transfer studies.[33] However, for the conformations of I and II observed in ZnTPP there is no correlation between the values of r and J. Thus, although there may be a dependence of J on r for direct overlap of the orbitals containing the unpaired electrons, there is no such relationship when the interaction is through a series of intervening orbitals as in I and II. It has also been reported that in titanium dimers with organic bridging ligands there was no correlation between the values of J and r.[34]

The EPR spectrum of I has also been examined in a frozen solution of toluene and THF.[5] Simulation of the spectra gave r = 13.5 Å, $\epsilon = 75°$, and $J = -40 \times 10^{-4}$ cm^{-1}.[5] The g and A values for the copper and nitroxyl electrons in the frozen solution were in good agreement with the values reported in Tables I and III. Other conformations may have been present in the frozen solution, but their presence was not detected. The values of r and J obtained from the frozen spectrum are different from the values obtained for any of the species in the ZnTPP single crystal. A powder sample of I in ZnTPP gave a poorly resolved spectrum, but the extent of the nitroxyl region of the spectrum clearly indicated that no conformation of I was present in which the spin-spin splitting of the nitroxyl lines was as large as that observed in the frozen solution spectrum in toluene-THF. Therefore it was concluded that the differences in the parameters obtained in the single crystal and in frozen solution were due to differences in the conformation of I in the two environments and not to difficulties in the analysis of the spectra. The differences in conformations in the two environments suggest that crystal packing forces in the host lattice may have a substantial impact on the detailed conformation of the spin-labeled linkage in these copper complexes.

Conclusions

Analysis of the single-crystal EPR spectra of spin-labeled copper complexes I and II doped into ZnTPP has given a detailed picture of the exchange and dipolar contributions to the spin-spin interaction. Four conformations of each isomer were observed. The magnitude of the exchange coupling constant, J, was strongly dependent on the conformation of the molecule and was larger for trans isomer I than for cis isomer II. The sign of J was positive for some conformations and negative for other conformations. There was no correlation between the value of J and the interspin distance, r.

There is an increasingly strong analogy between NMR nuclear coupling constants and EPR electron-electron coupling constants. It has been known for some time that the signs and magnitudes of NMR coupling constants are dependent on molecule conformation, but this study provides the clearest evidence to date that EPR coupling constants have a similar dependence. It is anticipated that further studies of EPR electron-electron coupling constants will become as important an aspect of EPR spectroscopy as nuclear coupling constants are in NMR.

Acknowledgment. This work was supported in part by NIH Grant GM21156.

Registry No. I, 76451-29-1; II, 76497-30-8; ZnTPP, 14074-80-7.

(26) Emsley, J. W.; Phillips, L.; Wray, V. *Prog. NMR Spectrosc.* **1978**, *10*, 83-756.
(27) Voegeli, U.; Philipsborn, W. *Org. Magn. Reson.* **1975**, *7*, 617-627.
(28) Prokofev, E. P.; Karpeiskaya, E. I. *Tetrahedron. Lett.* **1979**, 737-740.
(29) Ten Hoedt, R. W. M.; Van Koten, G.; Noltes, J. *G. J. Organomet. Chem.* **1979**, *170*, 131-149.
(30) Estaigh-Hosseini, H.; Kroto, H. W.; Nixon, J. F.; Brownstein, S.; Morton, J. R.; Preston, K. F. *J. Chem. Soc., Chem. Commun.* **1979**, 653-654.
(31) Coffman, R. E.; Buettner, G. R. *J. Phys. Chem.* **1979**, *83*, 2392-2400.
(32) McNally, J. M.; Kreilick, R. W. *Chem. Phys. Lett.* **1981**, *79*, 534-540.
(33) Stryer, L.; Thomas, D. D.; Meares, C. F. *Ann. Rev. Biophys. Bioeng.* **1982**, *11*, 203-222.
(34) Francesconi, L. C.; Corbin, D. R.; Clauss, A. W.; Hendrickson, D. N.; Stucky, G. D. *Inorg. Chem.* **1981**, *20*, 2059-2069.

Intermolecular Motional Degrees of Freedom of H_2O and D_2O Isolated in Solid Gas Matrices

Erich Knözinger* and Rüdiger Wittenbeck

Contribution from the Institut für Physikalische Chemie, Universität Siegen, D-5900 Siegen 21, Federal Republic of Germany. *Received August 4, 1982*

Abstract: Disordered solids of pure noble gases (Ar, Kr, Xe) as well as these matrices doped with H_2O and D_2O (1:1000) were studied by far-IR Fourier spectroscopy at very low temperatures (10 K). Previous neutron diffraction studies and the temperature dependence of the far-IR spectra measured in this study permit assignment of the IR-active phonon absorption of pure solid inert gas matrices. There is conclusive evidence that water introduced in these matrices at very low concentrations (1:1000) is present in the form of two fundamentally different species: (1) nearly freely rotating water molecules that have IR-active rotational transitions below 40 cm^{-1}, and (2) inert gas hydrates that contribute IR-active intermolecular vibrations between 40 and 100 cm^{-1}. In solid nitrogen the relevant spectral range is free of characteristic H_2O absorption, indicating that free rotation does not occur. The interaction between N_2 and H_2O gives rise to intermolecular vibrations located considerably above 100 cm^{-1}.

Far-infrared spectroscopic observations of polar and nonpolar molecules embedded in solid inert gas matrices promise to provide an extremely important tool for the study of intermolecular interactions. Experimental determination of the concentration and temperature dependence of the low-frequency bands enables intermolecular vibrations of aggregates to be distinguished from vibrations of the isolated monomer molecules relative to the cage. In addition, the character of the motion may be described

0002-7863/83/1505-2154$01.50/0

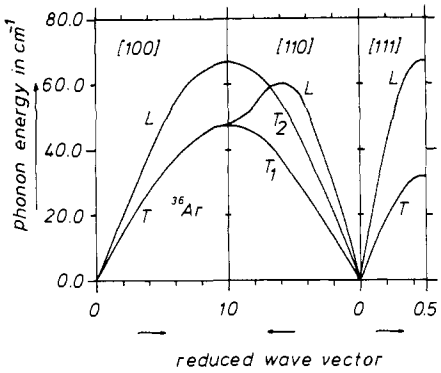

Figure 1. Phonon dispersion curves of ^{36}Ar along the three symmetry directions (L and T stand for longitudinal and transverse modes, respectively). These data were obtained from neutron diffraction experiments at 10 K. (The authors are greatly indebted to Prof. Dr. G. Schirane for this diagram.)

qualitatively by using isotope substitution of the dopant.[1-3]

The significance of some of the earlier studies[2,4-6] has been limited by uncertainties in the assignment of the phonon spectra of solid gas matrices and by the far-IR absorptions of possible impurities—particularly of H_2O—introduced into the matrix in the course of sample preparation.

These questions have been addressed in a study by Cugley and Pullin,[7] published about one decade ago. However, this study suffered from various instrumental drawbacks inherent in the technological state-of-the-art of that time. The availability of commercial periodic Michelson interferometers and He-cooled Ge bolometer detectors now greatly enhances the ease and reliability of studies in the 10–100-cm^{-1} spectral region. In an earlier study we were led to conclusions concerning Kr, none of which are now tenable.[2] In the present study we revise these results, providing much more definitive assignments for both the phonon spectra of pure solid inert gases and the intermolecular motions of isolated H_2O and D_2O in these matrices.

Experimental Section

The samples, H_2O and D_2O (Merck GmbH; stated isotopic purity of 99%), were freed of relatively volatile impurities be repeatedly freezing at 77 K and pumping on the solid sample. (To avoid a significant deuterium isotopic exchange, the vacuum system was optimized such that the leak and desorption rate amounted to less than 10^{-6} mbar L s^{-1}. In addition, the interior of the vacuum system was treated repeatedly with D_2O vapor.) The Ar, Kr, Xe, N_2 used as matrix gases (Messer Griesheim GmbH) had a stated purity of 99.9997% and were further dried by feeding them through a 3-m long copper pipe held at −120 °C. A glass vacuum system and standard manometric procedures were applied to produce the gas mixture of a molar ratio A/M (A = [sample], M = [matrix gas]) of 1:1000, which was deposited at a temperature of ~10.5 K (Ar, Kr, Xe) or 20 K (N_2) and at a deposition rate of 10 μmol/s. The quantity of H_2O or D_2O within the matrix amounted to less than 50 μmol.

All of the experiments were conducted by using an Air Products Model CSW-202 Displex closed-cycle helium refrigeration system. The pressure within the cryostat before cooling down amounted to 2×10^{-6} mbar. To anneal the sample, a temperature of 33 K (Ar), 46 K (Kr, Xe), and 30 K (N_2) was maintained for approximately 10 min. Unless otherwise stated, spectra were recorded at a sample temperature of 10 K. The far-IR spectra were recorded with a far-infrared Fourier spectrophotometer Model IFS-114 (Bruker Analytische Messtechnik GmbH) equipped with a He-cooled Ge bolometer working below the λ point. The beam splitter used had a specified thickness of 25 μm. The instrument was purged by a stream of dry air to remove water vapor. At the 1.0-cm^{-1} resolution used for these experiments, the accuracy and precision of the determination of band positions are estimated to be better than 0.5 cm^{-1} in most of the observations. All other experimental details are reported elsewhere.[1,3]

Table I. Energy Values (in cm^{-1}) for the Maximum Phonon Densities of States in Solid Ar, Kr, and Xe (Accuracy Better Than 2%)[a]

solid noble gas	position (cm^{-1}) of max phonon density of states at 10 K			
Ar	33.8	50.5	63.4	70.8
Kr	23.7	35.0	44.3	50.3
Xe	20.5	30.5	38.2	43.1

[a] The data were obtained from neutron diffraction measurements (ref 8–10).

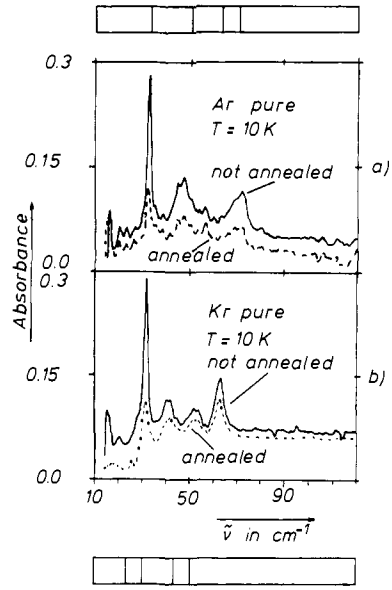

Figure 2. Far-IR spectra of pure solid Ar and Kr. The schematic spectra above and below are drawn to show the positions of the maximum phonon densities of states of these two noble gases.

Results

The dispersion curves of single crystals of Ar,[8] Kr,[9] and Xe[10] have been determined in neutron diffraction studies. An example (^{36}Ar) is given in Figure 1. On the basis of these dispersion curves, the positions of the maxima of the phonon density of states are evaluated in Table I with an accuracy of better than 2%. The resulting line spectra (schematic) of Ar and Kr are compared with the respective experimentally obtained far-IR spectra of the pure solid gases in Figure 2. (The solid is produced under matrix isolation conditions.) On annealing the matrix the intensity of all bands is reduced, particularly that of the sharp and intense bands at 32.4 cm^{-1} in Ar and at 31.6 cm^{-1} in Kr.

In contrast to impurities such as O_2, N_2, and CO_2, which do not alter the spectra to any measurable extent, H_2O as dopant dramatically enhances the intensity of all bands observed for pure solid Ar (Figure 3a,b). In addition the sharp band at 32.4 cm^{-1} experiences a considerable increase in the FWHM bandwidth (3.5 cm^{-1} vs. 2.0 cm^{-1}) and a slight shift to 33.1 cm^{-1}. As is shown in Figure 3b, on annealing different rates of change in intensity are observed; the intensities of peaks above 80 cm^{-1} vary only slightly, if at all, whereas the intensities of peaks below 80 cm^{-1}

(1) Knözinger, E.; Leutloff, D. *J. Chem. Phys.* **1981**, *74*, 4812–4818.
(2) Knözinger, E.; Wittenbeck, R.; Leutloff, D. *Opt. Eng.* **1982**, *21*, 553–556.
(3) Knözinger, E.; Wittenbeck, R. *Ber. Bunsenges. Phys. Chem.*, in press.
(4) Barnes, A. J.; Davies, J. B.; Hallam, H. E.; Scrimshaw, G. F. *J. Chem. Soc. D* **1969**, 1089–1090.
(5) Katz, B.; Ron, A.; Schnepp, O. *J. Chem. Phys.* **1967**, *46*, 1926–1929.
(6) Mason, M. G.; von Holle, W. G.; Robinson, D. W. *J. Chem. Phys.* **1971**, *54*, 3491–3499.
(7) Cugley, J. A.; Pullin, A. D. E. *Chem. Phys. Lett.* **1973**, *19*, 203–208.
(8) Fujii, Y.; Lurie, N. A.; Pynn, R.; Schirane, G. *Phys. Rev. B: Condens. Matter* **1974**, *B10*, 3647–3659.
(9) Skalyo, J., Jr.; Endoh, Y.; Schirane, G. *Phys. Rev. B: Condens. Matter* **1974**, *B9*, 1797–1803.
(10) Lurie, N. A.; Schirane, G.; Skalyo, J., Jr. *Phys. Rev. B: Condens. Matter* **1974**, *B9*, 5300–5306.

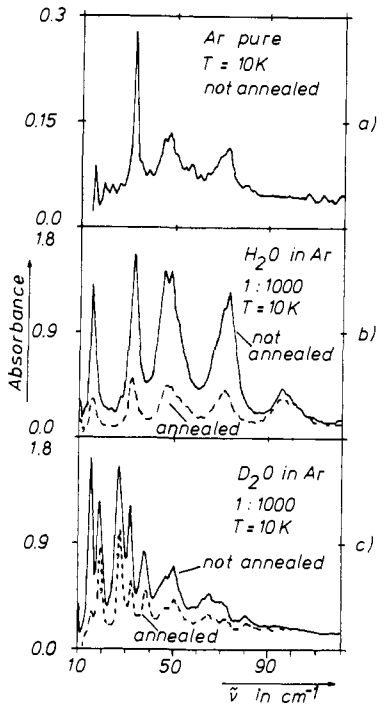

Figure 3. Far-IR spectra of H_2O (b) and D_2O (c) in solid Ar before and after annealing. For comparison the spectrum of pure Ar is given in a.

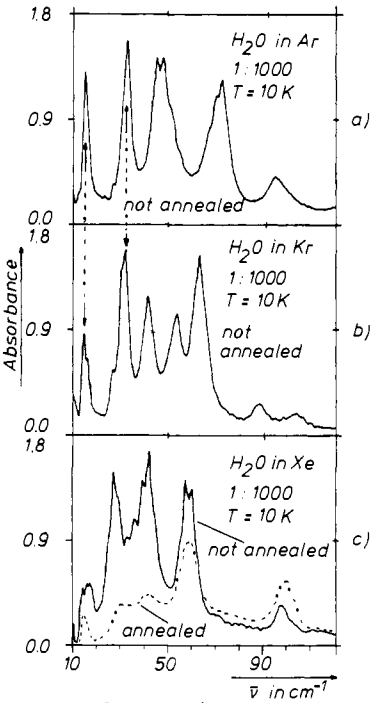

Figure 4. Far-IR spectra of H_2O in solid Ar (a), Kr (b), and Xe (c). For Xe the effect of annealing is also shown.

decrease markedly. When D_2O is added to the solid Ar (Figure 3c), the far-IR spectrum is completely different from that of H_2O under the same physical conditions, whereas the behavior on annealing is qualitatively the same for both isotopic species. In contrast to the H_2O spectrum, the D_2O spectrum has a sharp band at 32.4 cm^{-1} similar to that observed for pure solid Ar (Figure 3a–c).

On comparison of the influence of the different inert gases on the embedded H_2O (Figure 4), a most striking observation is made: below 40 cm^{-1} the spectra for Ar, Kr, and Xe as matrix gas are very similar—those for Ar and Kr are almost identical—whereas the spectral pattern above 40 cm^{-1} depends on the matrix material used. The behavior of the far-IR spectra of H_2O and D_2O in Kr

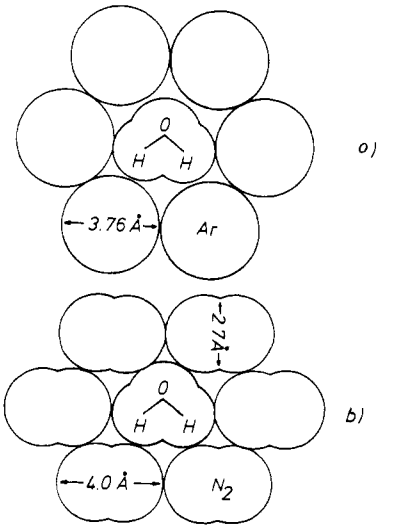

Figure 5. Schematic representation of a water molecule isolated in solid Ar (a) and N_2 (b).

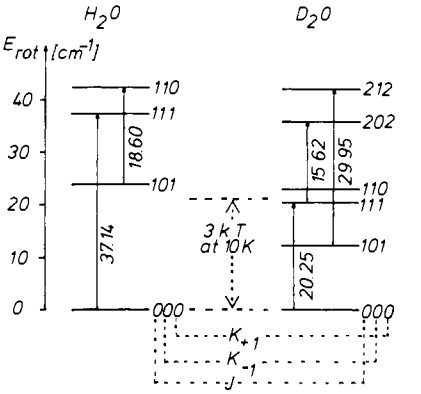

Figure 6. Energy level diagram for the rotational IR spectrum of H_2O and D_2O (J, K_{+1} and K_{-1} are rotational quantum numbers). The solid vertical arrows stand for the transitions which are experimentally observed for H_2O and D_2O isolated in solid noble gases at 10 K. (See ref 15 and 16. The authors are greatly indebted to Dr. D. Christen for computational work.)

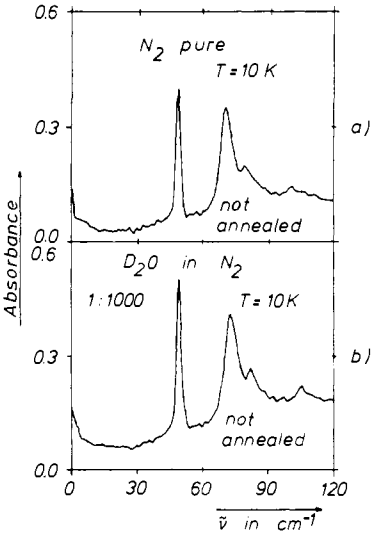

Figure 7. Far-IR spectra of pure solid N_2 and solid N_2 doped with D_2O.

and, particularly, in Xe on annealing differs from that in Ar. Different rates of intensity changes are found also in the spectral interval between 40 and 80 cm^{-1}.

The pure solid N_2 matrix has three absorption peaks in the range between 40 and 80 cm^{-1} (Figure 7a). This pattern shows little or no change (band shift of less than 2 cm^{-1}) on introducing H_2O

or D_2O (Figure 7b). No significant isotope effects are observed.

Discussion

An important requirement in all spectroscopic studies of solutions is that of optical transparency of the solvent in the spectral range of interest. The first task of the present investigation is, therefore, the study of the absorption characteristics of solid Ar, Kr, and Xe in the range between 10 and 100 cm^{-1}.

All of the phonon dispersion curves of the solid noble gases show only acoustic branches[8-10] which have vanishing phonon energy E_{phonon} for vanishing magnitude of the wave vector $\vec{k}$ (see, for example, dispersion curves of ^{36}Ar in Figure 1). Optical excitation of lattice vibrations in the form of first-order absorption processes requires the wave vectors of the incident photons and of the phonons created in the absorption process to be equal.[11] Consequently, only phonons of very small wave vector can be active in first-order absorption ($|\vec{k}| \rightarrow 0$). The phonon wave vector selection rule relates to single crystals, which evidently do not grow under matrix isolation conditions. On the contrary, during the deposition of the matrix gas on the cold surface at 10–20 K many lattice defects are introduced. The selection rule therefore no longer holds, and optical phonon excitation should be expected for finite wave vectors. This should occur with maximum probability at the positions of the maxima of the phonon density of states. These positions may be determined as the values of the phonon energy for which the respective dispersion curves have zero slope:

$$\frac{dE_{phonon}}{d|\vec{k}|} = 0 \qquad (1)$$

Following this procedure the data listed in Table I which show where phonon bands may occur if they are activated by lattice defects or impurities, are obtained.

The far-IR spectra of pure solid Ar and Kr deposited under matrix isolation conditions are, in fact, relatively complicated (Figure 2). They consist of a number of comparatively broad bands of low intensity and of one strong and sharp line (Ar, 32.4 cm^{-1}; Kr, 31.6 cm^{-1}; FWHM bandwidth, 2 cm^{-1} for Ar and Kr). This peak lies close to the position of a maximum of the phonon density of states for both Ar (33.8 cm^{-1}) and Kr (35.0 cm^{-1}) and should, unlike the other absorption bands, be attributed to a phonon excitation. (A FWHM bandwidth of 2 cm^{-1} for a phonon band of highly disordered pure solid Ar or Kr is, of course, surprising in view of the zero-slope criterion (eq 1). A possible explanation may be based on the presence of impurities (traces of H_2O) which are known to activate sharp phonon transitions.) Such an assignment is supported by the unique temperature dependence of these lines, which experience a reversible low-frequency shift and a reversible increase of the width at half-height as the temperature is increased (this effect is very small for Kr). Such behavior is characteristic of phonon bands.[12] The temperature rise, ΔT, must not amount to more than 8 K, in order to avoid annealing effects, which are related to a reduction of the influence of lattice imperfections and are, therefore, irreversible. The annealing procedure causes the phonon band in Ar and Kr to decrease in intensity considerably more rapidly than the other bands (Figure 2)—a fact which emphasizes that only one phonon band may be activated in both pure Ar and Kr by the lattice imperfections inherent in the physical conditions applied during the production of solid gas matrices. (In addition, other phonon bands—for example, the one at 70.8 cm^{-1} in Ar—appear in the far-IR spectrum, if strongly polar dopants, such as acetonitrile are introduced in solid noble gases.[1,3]) Another approach must be pursued to explain the remaining far-IR bands of solid Ar and Kr.

In spite of the high stated purity of the noble gases, the possibility cannot be completely excluded that traces of impurities are responsible for the unexplained far-IR absorptions of solid noble gases. Among the more likely impurities are the atmospheric gases, i.e., O_2, N_2, CO_2, or H_2O. When Ar and Kr matrices are doped with these impurities at an A/M ratio of 1:1000, no significant changes of the far-IR spectra are observed for O_2, N_2, and CO_2 whereas for H_2O all bands observed for the pure noble gas experience a dramatic increase in intensity (Figure 3a,b). The respective phonon bands also grow markedly in intensity and are considerably broadened. It must be assumed that an as yet unassigned water absorption is superimposed on the phonon band. In fact, the sharp phonon band reappears in Ar (Figure 3c) and in Kr when H_2O is replaced by D_2O. (It was not possible to specify the extent of HOD contamination since the instrument used did not cover the mid-IR spectral region. But from concentration-dependent studies it may be inferred that HOD does not contribute significantly to the absorption maxima observed in the course of the D_2O matrix studies.) Because all of the bands lose intensity on annealing, it is not possible to assign any of them to intermolecular vibrations of associated water molecules. During the annealing procedure the matrix becomes less rigid, making it possible for the H_2O molecules to diffuse together and to form aggregates. If the bands under consideration were due to intermolecular vibrations of associated molecules, their intensity should have increased rather than decreased on annealing. In addition, the positions of intermolecular vibrations of water dimers, already known from earlier studies,[13,14,15] are located above 100 cm^{-1}. The presence of multimers which are assumed to exhibit vibrational modes below 100 cm^{-1} is extremely unlikely at an A/M ratio of 1:1000. A high degree of isolation may thus be presumed for the H_2O molecules which contribute the far-IR spectrum in Figure 3b, and the observed transitions must be related to motions of the isolated H_2O molecules relative to the cage. Measurements in different matrices (Ar, Kr, Xe) may aid in the assignment of these motions (Figure 4) (intramolecular vibrational transitions of H_2O appear more than 1000 cm^{-1} above the spectral range under study). Below 40 cm^{-1} the spectra are very similar—for Ar and Kr almost identical—which means that the respective H_2O molecules move without any significant influence of the cage atoms. This, in turn, is only possible by assuming an almost free rotation of isolated H_2O molecules. The space required for a freely rotating H_2O molecule agrees satisfactorily with the dimensions of the smallest possible cage in Ar (Table II, Figure 5a). The rotational transitions in H_2O vapor at 10 K (=7 cm^{-1}) may be calculated.[16] Two of them, which are represented in the energy level diagram of Figure 6 by vertical arrows, agree relatively well with the positions (Table II) of the observed intense absorption bands below 40 cm^{-1}. Differences, particularly for H_2O in Xe, stem from the interaction of the rotating dipole of H_2O with the polarizable cage atoms. This interaction is certainly stronger for Xe than for Ar and Kr, since the polarizability[18] of Xe is extraordinarily high as compared

Table II. Band Positions of the Rotational Transitions of H_2O in Solid Ar, Kr, and Xe at 10 K, Represented Together with Characteristic Properties of the Noble Gas Matrices

noble gas M	cage dimensions,[a] Å	polarizability,[b] cm^3	band positions of H_2O in M, cm^{-1}
Ar	3.76	16.3×10^{-25}	15.2 33.1
Kr	4.00	24.8×10^{-25}	15.2 32.4
Xe	4.34	40.1×10^{-25}	14.5 27.3

[a] Data refer to the diameter of the largest sphere that normal cage spacings will accomodate (ref 19). [b] Reference 18.

(11) Loudon, R. *Proc. Phys. Soc.* **1964**, *84*, 379–388.
(12) Klein, M. L.; Venables, J. A. "Rare Gas Solids"; Academic Press: London 1976; Vol. 2, p 953.
(13) Mann, B.; Neikes, T.; Schmidt, E.; Luck, W. A. P. *Ber. Bunsenges. Phys. Chem.* **1974**, *78*, 1236–1241.
(14) Bentwood, R. M.; Barnes, A. J.; Orville-Thomas, W. J. *J. Mol. Spectrosc.* **1980**, *84*, 391–404.
(15) Knözinger, E.; Wittenbeck, R., unpublished.
(16) Helminger, P.; de Lucia, F. C. *J. Mol. Spectrosc.* **1978**, *70*, 263–269.
(17) Steenbeckeliers, G.; Bellet, J. *J. Mol. Spectrosc.* **1973**, *45*, 10–34.

with that of Ar and Kr (Table II), whereas the cage dimensions[19] are comparable for the three noble gases (variations of 10% from Ar to Kr and from Kr to Xe (Table II)). Similar observations were made for D_2O (calculated rotational spectrum; see ref 17), which gives rise to three strongly IR-active rotational transitions in solid noble gas matrices (Figures 3c and 6). Two of these transitions have already been observed and assigned in the way described here by Cugley and Pullin.[7] At that time the overlap of rotational transitions of H_2O and D_2O with phonon bands of the solid noble gas had not yet been recognized. Conclusions that H_2O and D_2O can experience essentially free rotation in solid rare gases were also drawn from earlier mid-IR studies by Redington and Milligan[20,21] and by Ayer and Pullin.[22,23] It may be argued against the assignment of H_2O and D_2O absorptions below 20 cm^{-1} as thermally excited bands (Figures 3 and 6) that their intensity is relatively high and that they do not exhibit the expected large intensity increase on warming the matrix moderately (e.g., to 15 K). These phenomena are most probably related to forbidden nuclear spin conversion[24] of the two protons and will be subject to a separate publication.

Above 40 cm^{-1} the far-IR spectra of H_2O and of D_2O in Ar, Kr, and Xe are completely dissimilar (Figure 4). The spectra are much more characteristic of the solid noble gas used than of the isotopic species of H_2O. Since the H_2O molecules are completely isolated, the bands between 40 and 80 cm^{-1} must be explained by the formation of stable heteroassociates of H_2O with the noble gas atoms. Thus, the observed peaks are the intermolecular vibrations of these noble gas hydrates. Some of these bands behave differently from the others on annealing. This is particularly true for Xe, for which each band shows a different rate of intensity change on annealing—a phenomenon which may be understood in terms of the presence of more than one Xe hydrate (Figure 4c). The same explanation most probably holds for the striking annealing behavior of the band at 94.7 cm^{-1} observed for H_2O in solid Ar (Figure 3b), even though an interpretation on the basis of a hot band of the 48-cm^{-1} fundamental or of a water multimer may not be completely excluded.

The most striking result of the present investigation is the unusually high intensity of the bands observed below 90 cm^{-1} on introducing H_2O molecules in solid noble gas matrix under physical conditions that favor a high degree of isolation. One of these physical conditions, and the most significant one, is a sufficiently low concentration. In the experiments described here, with an A/M ratio of 1:1000, this corresponds to an absolute amount of H_2O of less than 50 μmol, yielding band intensities of 1.5 absorbance units (Figure 4). The absorbance coefficients—estimated by assuming that only 10% of the 50 μmol of H_2O available for the experiment are deposited on the cold surface accessible to the far-IR radiation—amount to more than 10^4 L mol^{-1} cm^{-1}, which is exceptional in IR and far-IR spectroscopy. On annealing, aggregates are formed absorbing above 100 cm^{-1} with absorbance coefficients which are smaller by at least 2 orders of magnitude than those for isolated monomers. (If intermolecular vibrations of water associates are to be studied in the far-IR spectrum (>100 cm^{-1}), A/M ratios of the order of 1:100 to 1:50 have to be applied[13,14,15] to attain reasonable band intensities.) These observations support the given assignment of the bands below 90 cm^{-1}: the high absorbance coefficients refer to rotational and librational transitions of isolated H_2O molecules whose matrix elements depend upon dipole moments whereas vibrational transitions depend on dipole derivatives. When self-association occurs, the rotational or librational motions of the isolated molecules become constrained to librational movement in the associated complex with substantially reduced amplitudes and, therefore, substantially reduced transition probabilities.

H_2O and D_2O introduced into a N_2 or a CH_4 matrix under physical conditions comparable to those applied for the noble gases do not absorb at all below 100 cm^{-1}. In solid N_2 the impurity H_2O or D_2O (Figure 7) causes only a slight shift of the bands at 49.0 and 70.8 cm^{-1} which, on the basis of the temperature dependence, have been assigned to lattice vibrations. No free rotation takes place—a fact which is intuitively to be expected for N_2 as matrix material when the dimensions of the cage and of the H_2O molecule are compared (Figure 5b). No intermolecular vibrations of hydrates comparable to the noble gas hydrates occur. Instead, in a N_2 matrix H_2O absorptions appear at 147 and 225 cm^{-1} which have been assigned to librations of isolated H_2O molecules.[14] H_2S isolated in solid Ar under the same conditions as for the water studies does not exhibit any significant absorption between 10 and 100 cm^{-1}, nor does absorption appear when the H_2S concentration is increased by a factor of 10. In contrast to H_2O, H_2S is, apparently, not able to perform a nearly free rotation or to form heteroassociates comparable to the noble gas hydrates. These points emphasize the need for further studies in order to define the factors which influence the motion of small molecules such as H_2O and H_2S isolated in solid matrices.

Conclusion

An important requirement which must be met in far-IR matrix isolation spectroscopy in the spectral range below 100 cm^{-1} is the efficient elimination of traces of water vapor in the sample, in the inert gas, in the cryostat, and in the vacuum systems applied. With the precautions adopted in the course of the present investigation, which was performed in a glass vacuum system, it is possible to suppress the final water content in the solid noble gas matrix to an approximate value of $\sim 1:10^5$, which guarantees maximum absorbance values due to traces of H_2O impurities of ~ 0.05 absorbance units and less in the spectral interval below 80 cm^{-1}. Studies of the intermolecular motion of molecules other than water in solid noble gas matrix may reliably be performed and interpreted under these conditions[1,3] without the need to use an expensive metal ultrahigh vacuum system.

It is important to remember that phonon bands which are not IR active in the pure solid noble gas matrix, even for high concentrations of lattice imperfections, may well be activated by strongly polar dopants such as CH_3CN[1] and HCN.[3] Therefore, the assignment must be carefully checked whenever an absorption is located close to the position of a maximum phonon density of states (Table I).

Acknowledgment. We thank Prof. Dr. H. D. Lutz (Universität Siegen), who provided the Michelson interferometer for the studies described above. Thanks are also due to Dr. M. Jacox (NBS, Washington) for revising the manuscript and to Prof. Dr. H.-J. Jodl (Universität Kaiserslautern) for valuable comments and suggestions. The financial support of Deutsche Forschungsgemeinschaft and of Fonds der Chemischen Industrie is gratefully acknowledged.

Registry No. H_2O, 7732-18-5; D_2O, 7789-20-0; Ar, 7440-37-1; Kr, 7439-90-9; Xe, 7440-63-3; N_2, 7727-37-9.

(18) Schuster, P. *Angew. Chem.* **1981**, *93*, 532–553.
(19) Hallam, H. E., Ed. "Vibrational Spectroscopy of Trapped Species"; Wiley: London, 1973; p 51.
(20) Redington, R. L.; Milligan, D. E. *J. Chem. Phys.* **1962**, *37*, 2162–2166.
(21) Redington, R. L.; Milligan, D. E. *J. Chem. Phys.* **1963**, *39*, 1276–1284.
(22) Ayers, G. P.; Pullin, A. D. E. *Spectrochim. Acta, Part A* **1976**, *32A*, 1629–1639.
(23) Ayers, G. P.; Pullin, A. D. E. *Spectrochim. Acta, Part A* **1976**, *32A*, 1641–1643.
(24) Ayers, G. P.; Pullin, A. D. E. *Ber. Bunsenges. Phys. Chem.* **1978**, *82*, 62–63.